

An observational study of the association among interatrial adiposity by computed tomography measure, insulin resistance, and left atrial electromechanical disturbances in heart failure

Chung-Lieh Hung (MD, MSc)^{a,b,c,d,e}, Chun-Ho Yun (MD)^f, Yau-Huei Lai (MD)^{a,b,c,d}, Kuo-Tzu Sung (MD)^{a,b,c,d}, Hiram G. Bezerra (MD)^g, Jen-Yuan Kuo (MD)^{a,b,c}, Charles Jia-Yin Hou (MD)^{a,b,c}, Tze-Fan Chao (MD)^h, Bernard E. Bulwer (MD)ⁱ, Hung-I. Yeh (MD, PhD)^{a,b,c,d}, Shou-Chuan Shih (MD)^j, Shing-Jong Lin (MD, PhD)^{k,*}, Ricardo C. Cury (MD)^l

Abstract

Excessive visceral adiposity, hypothesized to be a key mediator in metabolic derangements, has recently been shown to exert toxic effects on cardiac structure and function. Data regarding the mechanistic link between regional adiposity, left atrial (LA) electromechanical remodeling, and heart failure with preserved ejection fraction (HFpEF) have been lacking.

Various visceral adiposity measures, including pericardial fat (PCF), thoracic periaortic (TAT) fat, regional inter-atrial fat (IAF), and atrioventricular groove fat (AV Groove Fat), were assessed by multidetector computed tomography in 2 study cohorts (an annual health survey cohort and an outpatient cohort). We related such measures to cardiometabolic profiles in health survey cohort and LA electromechanical indices in our outpatient cohort, with Cox proportional hazards performed to examine the temporal trends of heart failure (HF).

In our annual health survey cohort (n=362), all 4 adiposity measures were positively related to unfavorable anthropometrics and systemic inflammation (high-sensitivity C-reactive protein) (all $P < 0.05$). In addition, both greater IAF and AV Groove Fat were positively associated with higher fasting glucose, HbA1c levels, and insulin resistance (all $P < 0.05$). In the outpatient cohort, the HFpEF group demonstrated the greatest adiposity measures, with greater IAF (≥ 8.2 mm, hazard ratio: 4.11, 95% confidence interval: 1.50–11.32) associated with reduced LA strain (β -coef: -0.28), higher LA stiffness (β -coef: 0.23), and longer P wave duration (β -coef: 0.23) in multivariate models (all $P < 0.05$), and further related to higher HF hospitalization during follow-up.

We therefore propose a possible pathophysiologic link among greater visceral adiposity, systemic inflammation, cardiometabolic risks, and HFpEF. Regional adiposity, especially IAF, was tightly linked to altered LA electromechanical properties and likely plays a key role in HF prognosis.

Abbreviations: AF = atrial fibrillation, AV Groove Fat = atrio-ventricular Groove Fat, HFpEF = heart failure with preserved ejection fraction, IAF = Inter-atrial fat, LA = left atrial/left atrium, MDCT = multidetector computed tomography, PCF = pericardial fat, TAT = thoracic periaortic fat.

Keywords: cardiometabolic profiles, electromechanical, heart failure, strain, visceral adiposity

Editor: Celestino Sardu.

Funding: This work was partially funded by grants from National Science Council (NSC-101-2314-B-195-020, NSC 103-2314-B-010-005-MY3, 103-2314-B-195-001-MY3, 101-2314-B-195-020-MY1, MOST 103-2314-B-195-006-MY3), Mackay Memorial Hospital (10271, 10248, 10220, 10253, 10375, 10358, E-102003) and Taiwan Foundation for geriatric emergency and critical care.

Supplemental Digital Content is available for this article.

The authors report no conflicts of interest.

^a Department of Internal Medicine, Division of Cardiology, Mackay Memorial Hospital, Taipei, ^b Department of Medical Research, ^c Department of Medicine, Mackay Medical College, New Taipei City, Taiwan, ^d Mackay Junior College of Medicine, Nursing and Management, New Taipei City, ^e Institute of Clinical Medicine, and Cardiovascular Research Center, National Yang-Ming University, ^f Department of Radiology, Mackay Memorial Hospital, Taipei, Taiwan, ^g Cardiovascular Department, University Hospitals Case Medical Center, Cleveland, OH, ^h Department of Medicine, Division of Cardiology, Taipei Veterans General Hospital, Taipei, Taiwan, ⁱ Noninvasive Cardiovascular Research, Cardiovascular Division, Brigham and Women's Hospital, Boston, MA, ^j Department of Internal Medicine, Division of Gastroenterology, Mackay Memorial Hospital, ^k Department of Medical Research and Education, Taipei Veterans General Hospital, Institute of Clinical Medicine, and Cardiovascular Research Center, National Yang-Ming University, Taipei, Taiwan, ^l Cardiovascular MRI and CT Program, Baptist Cardiac Vascular Institute, Miami, FL.

* Correspondence: Hung-I. Yeh, Department of Internal Medicine, Division of Cardiology, Mackay Memorial Hospital, Mackay Medical College, New Taipei City 252, Taiwan (e-mail: hiyeh@ms1.mmh.org.tw); Prof. Shing-Jong Lin, Department of Medical Research and Education, Taipei Veterans General Hospital, Taipei, Taiwan 112, Republic of China (e-mail: sjlin@vghtpe.gov.tw).

Copyright © 2016 Wolters Kluwer Health, Inc. All rights reserved.

This is an open access article distributed under the terms of the Creative Commons Attribution-Non Commercial-No Derivatives License 4.0 (CCBY-NC-ND), where it is permissible to download and share the work provided it is properly cited. The work cannot be changed in any way or used commercially.

Medicine (2016) 95:24(e3912)

Received: 15 October 2015 / Received in final form: 14 May 2016 / Accepted: 18 May 2016

Published online 1 May 2016

<http://dx.doi.org/10.1097/MD.0000000000003912>

1. Introduction

Preserved left atrial (LA) mechanical function is critical in maintaining adequate cardiac filling and pump function in subjects in sinus rhythm. Deteriorating LA function is a key feature in the diagnosis of heart failure (HF) with preserved ejection fraction (HFpEF),^[1] and may be a clinical prognosticator in this patient population.^[2] Previous studies have demonstrated that chronically elevated left ventricular (LV) filling pressures may not fully explain LA mechanical failure or remodeling.^[3,4] Instead, several comorbid conditions including diabetes, obesity, hypertension, or coronary artery disease can contribute to LA fibrotic changes^[3] and shared common clinical features with HFpEF, which can be identified by lower values of LA deformation.^[5]

Hypertension-induced mechanical stretch can lead to ventricular remodeling and hypertrophy, as well as atrial enlargement and fibrosis,^[6] resulting in HF. However, metabolic derangements such as obesity and diabetes can cause HF,^[7] driven in part by the number of inflammatory signaling pathways superimposed on mechanical load.^[8–10] In addition, both metabolic disorders and systemic inflammation are linked to the onset of atrial fibrillation (AF).^[11]

Effective therapeutic approaches for patients with HFpEF remain limited,^[12] and further exploration of the pathophysiological mechanisms and pathways involved is therefore needed with a clinical perspective to more effective delivery of therapies. A recent focus is the role of visceral adipose tissue as a key player with important proinflammatory and biological mediators associated with adverse cardiac electromechanical remodeling and subclinical contractile dysfunction.^[13–15]

Therefore, we thus speculated that visceral adiposity, especially that in anatomic proximity to cardiac structures, not only plays a central role in mediating inflammation and oxidative stress, but may also trigger certain cardiac electromechanical disturbances that are more accentuated in HFpEF.

2. Methods

2.1. Study populations

This study consisted of 2 phases. The first phase of study comprised a cohort of patients who underwent annual health check-ups ($n=362$, from January 2007 to August 2009). All participants had routine physical examinations with baseline demographic and anthropometric information obtained, as well as detailed review of medical history. Biochemical data, routine body surface electrocardiography (ECG), and computed tomography (CT) were performed for cardiovascular disease characterization with subspecialty referral if appropriate. For the second phase of the study, we consecutively enrolled study subjects from the cardiovascular outpatient clinic ($n=206$, from January 2010 to July 2011) at a tertiary care hospital in North Taiwan (Mackay Memorial Hospital). Similarly, all participants underwent anthropometric measures with biochemical data collected. Routine ECG, echocardiography, and CT were also performed, and the aim was to validate the associations between CT-defined visceral adiposity and clinical cardiovascular risk profiles, and to further examine whether such adiposity measures may discriminate individuals with high cardiovascular risks or those with clinical evidence of HF.

For both study phases, body fat composition was assessed by utilizing bioelectrical impedance analysis from foot-to-foot impedance estimate using the Tanita-305 Body-Fat Analyzer

(Tanita Corp, Tokyo, Japan), which provided information about whole body fat percentage in the standing position. For the second phase of study, we further categorized them into healthy, co-morbidity, and HFpEF groups. The final subjects enrolled comprised those with known cardiovascular comorbidities ($n=108$) and those who had HFpEF ($n=58$). The details of study enrollment, including the definition of HF, eligibility, and exclusion criteria were similar to those used in our previous publication^[16]; an additional 40 subjects without previous diagnosis of any systemic disease in annual health check-ups served as the healthy control group. The comorbidities group was defined as those with any of the following clinical conditions: hypertension, diabetes, obesity (defined as body mass index [BMI] ≥ 30 kg/m²), minor degree of renal insufficiency (defined as estimated glomerular filtration rate [eGFR] < 60 mL/min/1.73 m²), history of cardiovascular diseases (stroke or coronary artery disease), or any medication use for hyperlipidemia. This study design was approved by the local ethics committee in accordance with the Declaration of Helsinki (12MMHIS052).

2.2. CT-defined visceral adiposity: PCF, TAT, IAF, and AV groove adipose tissue quantification

Multidetector CT (MDCT) study was performed using a Dual Source CT scanner (Somatom Definition, Siemens Medical Solutions, Forchheim, Germany) with 32×0.6 mm per tube with double sampling by z-flying focal spot, rotation time of 330 ms, tube voltage of 120 kV, and full tube current of 625 mA per tube (independent of patient size).

Contrast injection (iopamiro 370 mg/mL, Bracco, Italy) was administered (60–85 mL) at an injection rate of 5 mL/s with a delay calculated during the timing bolus scan. Overlapping transaxial images were reconstructed using a medium sharp convolution kernel (B2.5f) with an image matrix of 512×512 pixels, slice thickness and increment of 0.75/0.4 mm using an ECG-gated half-scan algorithm. Image reconstruction was retrospectively gated to ECG. Reconstructed image data were transferred to a dedicated workstation (Aquarius 3D Workstation, TeraRecon, San Mateo, CA) for subsequent visceral adipose tissue, pericardial fat (PCF), and thoracic periaortic (TAT) analyses. The semiautomatic segmentation technique was developed for quantification of fat volumes. We traced the region of interest manually and defined fat tissue by using Hounsfield units (HU) as pixels with the attenuation of -190 to -30 HU, which corresponded to adipose tissue in contrast-enhanced cardiac CT scans.^[17] PCF was defined as any adipose tissue volume (unit: mL) located within the pericardial sac (Fig. 1A). TAT tissue was defined as volume (unit: mL) of the adipose tissue surrounding the thoracic aorta, which extended 67.5 mm from the level of the bifurcation of pulmonary arteries as start point, with cranial-caudal coverage of the thoracic aorta to the diaphragm as its lower anatomical limit (Fig. 1B). For acquiring the thickness of regional epicardial adipose tissue (unit: mm), we further adjusted the imaging plane into horizontal long-axis plane for the measurements of inter-atrial fat (IAF) and atrioventricular (AV) groove fat (Fig. 1C). This approach has been validated previously.^[18]

We categorized the participants into 3 groups based on metabolic scores as defined by NCEP ATP III criteria^[19,20]: waist circumference ≥ 80 cm for women or ≥ 90 cm for men (1 point); serum fasting glucose concentration ≥ 100 mg/dL (≥ 5.5 mmol/L) (1 point); serum high-density lipoprotein (HDL) level < 40 mg/dL (< 1.03 mmol/L) for men or < 50 mg/dL (< 1.29 mmol/L) for

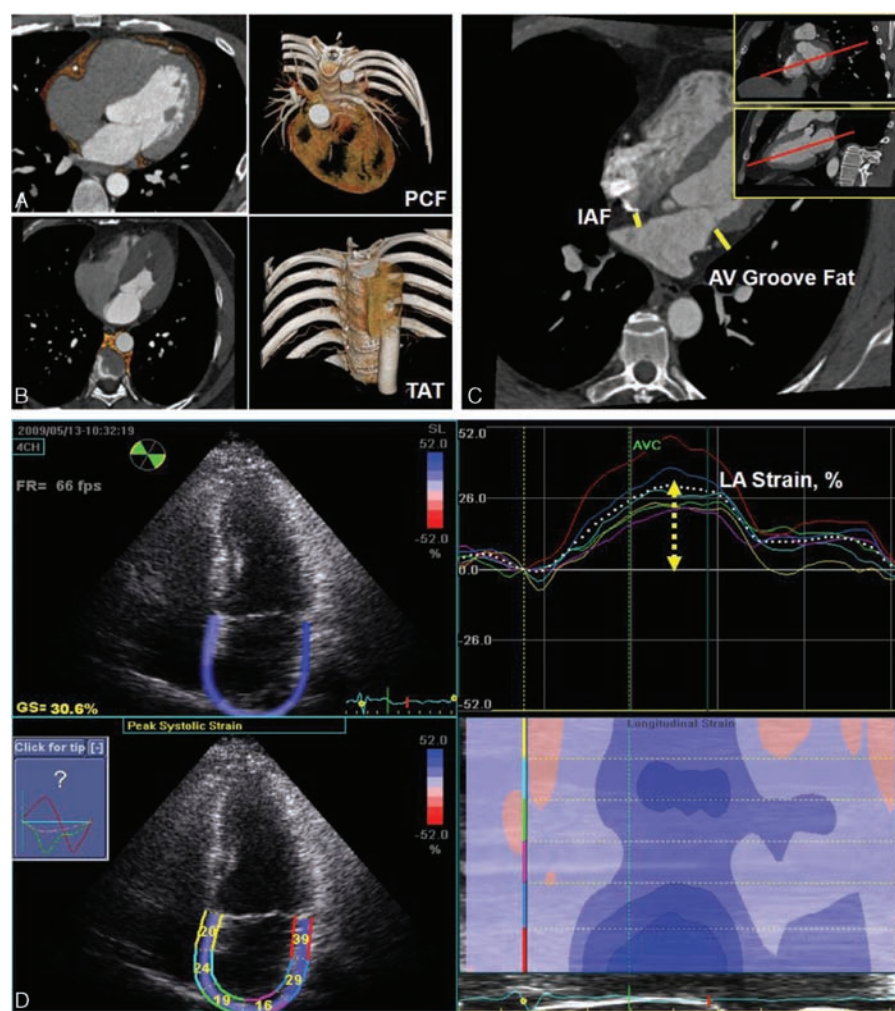


Figure 1. (A, B) Measurements of total volume of peri-cardial fat tissue (PCF) and thoracic periaortic fat tissue (TAT). Orange color indicated PCF and TAT in axial, sagittal, coronal views, and 3-dimensional reconstructions. (C) Thickness of PCF in interatrial septum (solid line) and left atrioventricular groove (dotted line) was measured in the horizontal long-axis view. (D) Left atrial (LA) deformation (LA strain, %) analysis by using 2-dimensional speckle-tracking technique and corresponding curves were displayed.

women (1 point); serum triglyceride level >150 mg/dL (>1.69 mmol/L) (1 point); and/or blood pressure $>130/85$ mmHg (1 point). The metabolic score therefore ranged from 0 to 5 with metabolic syndrome (MetS: defined as metabolic scores ≥ 3) denoting higher risk for cardiometabolic profiles, which had been shown to confer higher cardiovascular risks including HF in previous studies.^[10] Owing to a graded increase of cardiovascular diseases risk based on previous research,^[21] we therefore categorized our study population in protocol 1 as metabolic score 0 (reference category); metabolic scores 1–2; and metabolic scores ≥ 3 , defined as MetS.

2.3. Echocardiography protocol for assessing conventional echocardiography parameters and diastolic indices

Transthoracic Doppler echocardiography examination was performed on all subjects using a commercially available ultrasound system (Vivid 7, GE Vingmed Ultrasound, Horten, Norway) equipped with a 2 to 4 MHz transducer (M4S). Parameters including LA diameter, LV internal diameter, derived LV mass, and LV mass index were determined from M-mode measurements using American Society of Echocardiography

criteria.^[21] The aortic root diameter was defined as the largest end-diastolic diameter measured on the parasternal long-axis view.

LV end-diastolic and end-systolic volumes were further quantified using the biplane Simpson method with ratio of LV mass to volume calculated using LV mass divided by LV end-diastolic volume. Assessment of LV diastolic function was determined using pulsed-wave Doppler of transmitral inflow velocities measured at the tip of the mitral leaflets with E/A ratio assessed from early (E) and late diastolic (A) filling velocities. Tissue Doppler imaging was used to determine the lateral mitral annular velocities, measuring both the peak systolic (S') and early diastolic (E') values. Left-sided ventricular filling pressures (E/E') were estimated using the ratio of the early (E) transmitral Doppler velocity divided by the tissue Doppler imaging-derived early diastolic (E') lateral mitral annular velocity.

2.4. Assessment of systolic myocardial mechanics and LV twist by speckle-tracking deformation imaging

Baseline 2-dimensional images (including 2-chamber, 4-chamber, and apical long-axis views) for longitudinal strain and 3 short-axis views (including mitral, papillary, and apical levels) were

analyzed by offline endocardial border manual tracing, using novel offline proprietary software (EchoPAC version BT11 workstation; GE VingMed Ultrasound) based on automated speckle-tracking algorithms with an average frame rate estimated between 60 and 80 frames/s. The global longitudinal strain was averaged from all 3 apical views (2-chamber, 4-chamber, and apical long-axis views) and displayed parametrically as a polar plot (bull's-eye) map, with global circumferential and radial strain curves obtained by averaging different values from 3 different short-axis levels, respectively. Cardiac twist was generated automatically using the same software.

2.5. Assessment of LA electromechanical functions

The maximal and minimal LA volumes were calculated from apical 4-chamber and 2-chamber views just before mitral valve opening, and at mitral valve closure using the modified biplane 2-dimensional echocardiography (Simpson's method). During image acquisition, care was taken to optimize visualization of the LA cavity and to maximize LA area in apical views, avoiding foreshortening of the left atrium. We further assessed LA longitudinal systolic mechanical function (LA strain) by using same offline workstation as LV 2-dimensional speckle-tracking analysis from both apical 4- and 2-chamber views by the same technician. Briefly, the LA endocardial border was manually traced at end-systole using a point-and-click approach in both apical views. An epicardial surface tracing was automatically generated by the software, delineating a region of interest including 6 segments. The region of interest was manually adjusted to encompass the thickness of the LA myocardium, and an automated segmental tracking quality analysis was obtained (Fig. 1D). Minimal manual adjustment of the region of interest was performed in the case of segments with inadequate tracking with cine loop preview used to confirm that the inner tracking border followed the LA endocardial border throughout the cardiac cycle. The actual LA strain was derived as the average values of peak systolic strain of all LA segments during LV systole (Fig. 1D).

Participants underwent routine 12-lead surface ECG studies by using autonomic instruments (Page Writer Trim III, Phillip, 3000 Minuteman Road, Andover, MA) with standard settings (25 mm/s, 1 mV/cm, and 100 Hz) recorded for further analysis. Electrical parameters including QRS or PR duration, and QT interval (with or without correction for cycle length) were all obtained by automatic software algorithm across the 12-lead tracing. Quantitative assessments of P wave duration were performed by using DICOM format image analysis software (Sante DICOM editor, 3.1.20) with the nearest 4 ms as possible. In total, 2 P wave duration parameters, including original P wave maximum duration and corrected P wave maximum duration (corrected for heart rate based on Bazett's formula as: $P \text{ wave maximum duration} / [RR]^{1/2}$) from lead II, were evaluated in each study participant.^[21]

2.6. Agreement of LA volume measures between computed tomography and its association with LA strain

In total, 59 subjects, including 13 subjects from the normal population, 35 subjects from comorbidity, and 11 subjects from HFpEF groups were randomly chosen to have an echocardiography-derived LA volume measurement (Biplane Simpson's method) during end-systolic phase (with maximal LA volume) compared with the CT-defined LA volume measurement. The correlation between these 2 measures in our laboratory was good ($r=0.94$, $P<0.001$) with limits of agreement estimated to be: -1.586 to 15.416 by Bland-Altman analysis.

2.7. Statistical analysis

Continuous data are reported as the mean \pm standard deviation (SD) and compared using a nonparametric trend test (Wilcoxon rank sum test) across ordered age groups with categorical or proportional incidence data expressed as a proportion and compared with use of the χ^2 or Fisher exact test, as appropriate. One-way analysis of variance (ANOVA) was performed to test the differences in the continuous data among the 3 groups with a post hoc Bonferroni correction for paired comparisons. Because LA dysfunction and remodeling depend largely on age and other cardiovascular risk factors, an analysis of covariance was also used to adjust for relevant covariates in the comparison of mean values among the 3 groups. The minimum required samples needed to detect significant difference between the HFpEF and comorbidity groups by longitudinal LA deformation (strain), a sensitive and powerful clinical marker for such purpose, was calculated. A reported mean \pm SD of 19.9 ± 7.3 in the HFpEF group and 30.8 ± 11.4 in the asymptomatic LV diastolic dysfunction group with similar distribution of morbidities as in our comorbidity group resulted in an effect size (Cohen's d) of 0.563.^[22] Given that the subjects with HFpEF had a smaller amount with a potentially wide range of longitudinal strain value compared with asymptomatic subjects with clinical comorbidities (26%–34%), the authors prespecified the ratio as a 2:1 allocation ratio, leading to a sample size of nearly 80:40 for c-morbidity and HFpEF groups, respectively, with a power of 90% and a rate of 5%. The sample size calculation was performed by using G*Power 3.1.5 (University Kiel, Kiel, Germany). Additionally, a normal control group was included to contrast the difference from the comorbidity and HFpEF groups. Furthermore, to eliminate the possible influences of age, BMI, and sex distribution on visceral adiposity burden, cardiac deformation, and LA functional measures, we performed a subgroup matching of these variables and conducted paired comparisons among groups. To develop a standardized measure on the effects of various kinds of adiposity (PCF, TAT, AV Groove Fat, and IAF) on cardiac electromechanical functions, a z score was generated by subtracting the mean from each adiposity raw data and then dividing the difference by the SD. A multivariable regression model was used to determine the significance of the covariate-adjusted relation between LA deformation data and various periatrial adiposity, clinical variables, biochemical profiles, and echocardiography-derived measurements of LV mass with individual odds ratios, and P values and 95% confidence intervals (CIs) are reported. Cox proportional hazards ratio on temporal changes of HF admission rates was performed in our outpatient cohort, which aimed to explore the association between adiposity on clinical events, with most echocardiography-derived key parameters as confounders.

All data were analyzed with use of the STATA 9.0 software package (StataCorp). The P value was set for 2-tailed probability with a P value <0.05 considered statistically significant.

3. Results

3.1. The association between various adiposity measures and cardiometabolic profiles in subjects who underwent annual health survey.

The 362 participants (mean age: 51.7 ± 8.9 years old, 31% female sex) enrolled from annual health evaluation in the first phase of the study (January 2007–August 2009) were further categorized

into 3 different groups based on the metabolic scores (0, 1–2, ≥ 3). Greater metabolic scores were associated with older age, higher BMI, increased body weight, larger waist circumference, and higher blood pressures (Supplemental Material, Table 1, all trend $P < 0.05$, <http://links.lww.com/MD/B34>). In addition, a variety of cardiometabolic derangements, including increased fasting glucose concentrations, higher HbA1c levels, elevated triglyceride levels, greater insulin resistance, lower HDL, and worse renal function, were all related to higher metabolic scores (all trend $P < 0.05$). Higher metabolic scores are also associated with greater amount of body fat composition, visceral adiposity, and more elevated serum high-sensitivity C-reactive protein (hs-CRP) level (all trend $P < 0.05$).

Larger amounts of visceral fat (PCF, TAT, AV Groove Fat, and IAF) were associated with several unfavorable cardiometabolic profiles including greater body weight, elevated BMI, greater body fat composition, higher systolic blood pressure, and larger waist circumference (all $P < 0.05$) (Supplemental Material, Table 2, <http://links.lww.com/MD/B34>). In addition, larger AV Groove Fat and IAF were positively associated with higher triglycerides, HbA1c, insulin resistance (homeostatic model assessment-insulin resistance [HOMA-IR]), and higher systemic inflammation marker (hs-CRP), but were inversely associated with HDL level (all $P < 0.05$). A positive linear relationship between AV Groove Fat, IAF, and P wave duration by body surface ECG ($r = 0.14$ and $r = 0.23$ for AV Groove Fat and IAF, respectively, both $P < 0.05$) was also observed.

3.2. The feasibility and diagnostic accuracy of various adiposity measures for MetS

We further explored the clinical cut-off and diagnostic feasibility of these various sites of adiposity in identifying MetS (Supplemental Material, Table 3, <http://links.lww.com/MD/B34>). The PCF yielded the highest sensitivity (77.8%) (cutoff value: 76.2 mL, area under the receiver-operating characteristic [AUROC]: 66%, 95% CI: 0.60–0.71), and the IAF showed relatively high specificity (77.2%) (cutoff value: 6.6 cm, AUROC: 64%, 95% CI: 0.58–0.70) in identifying MetS. Meanwhile, IAF showed highest positive predictive value (39.4%), and PCF showed highest negative predictive value (89.29%) for MetS diagnosis.

3.3. Baseline demographic data and visceral adiposity in healthy, co-morbidity, and HFpEF groups from outpatient clinic

The study participants from the cardiovascular outpatient clinic in the phase 2 study (from January 2010 to July 2011) are reported in Table 1. Compared with healthy and comorbidity groups, subjects in the HFpEF group tended to be older with a higher female percentage, had greater BMI, and higher blood pressure (Table 1, all $P < 0.05$). Subjects in the comorbidity and HFpEF groups also had higher fasting glucose levels, whereas the HFpEF group presented with much worse renal function in terms of lower eGFR, together with higher metabolic scores (all $P < 0.05$). There was a trend toward higher hs-CRP and brain

Table 1

Baseline demographic information and various visceral adiposity measures in healthy, comorbidity, and HFpEF groups (n=206).

	Healthy group (N = 40)	Co-morbidity group (N = 108)	HFpEF group (N = 58)	P (trend) or χ^2
Baseline characters				
Age, y	53.95 ± 9.67	55.60 ± 10.49	64.33 ± 12.42 ^{*,†}	<0.001
Sex (female), %	16 (40.0%)	35 (32.4%)	31 (53.4%)	0.031
Weight, kg	64.88 ± 10.97	72.42 ± 15.27	70.46 ± 14.25	0.06
BMI, kg/m ²	23.59 ± 2.71	26.46 ± 3.94 [*]	27.18 ± 3.68 [*]	<0.001
Systolic blood pressure, mmHg	117.25 ± 10.81	132.49 ± 16.91 [*]	143.53 ± 14.07 ^{*,†}	<0.001
Diastolic blood Pressure, mmHg	69.63 ± 8.48	79.54 ± 10.80 [*]	78.21 ± 10.54 [*]	<0.001
Biochemical data				
Fasting glucose, mg/dL	98.28 ± 8.63	114.84 ± 28.28 [*]	125.07 ± 49.23 [*]	<0.001
Triglyceride, mg/dL	119.08 ± 66.55	140.33 ± 81.22	124.78 ± 65.90	0.716
HDL, mg/dL	50.84 ± 13.05	47.84 ± 14.75	44.55 ± 12.60	0.005
eGFR, mL/min/1.73m ²	97.56 ± 13.10	92.97 ± 25.50	77.89 ± 17.70 ^{*,†}	<0.001
Metabolic score	0.97 ± 1.04	2.27 ± 1.26 [*]	2.61 ± 0.98 ^{*,†}	<0.001
hs-CRP, mg/dL (median, 25 th –75 th)	0.087 (0.04–0.13)	0.19 (0.1–0.35) [*]	0.35 (0.12–0.91) ^{*,†}	<0.001
BNP (median, 25 th –75 th)	33.8 (15.8–50.5)	44.5 (20.9–61)	264.4 (226.1–320) ^{*,†}	<0.001
Medical history				
Hypertension history, %	0 (0%)	83 (76.9%)	43 (74.1%)	<0.001
Diabetes history, %	0 (0%)	32 (29.6%)	19 (32.8%)	<0.001
Hyperlipidemia history, %	0 (0%)	45 (44.1%)	33 (66%)	<0.001
Cardiovascular disease, %	0 (0%)	24 (22.2%)	8 (13.8%)	0.004
Various adiposity measures				
Body fat composition, %	25.4 ± 7.6	30.7 ± 7.6 [*]	35.1 ± 8.4 ^{*,†}	<0.001
PCF, mL	59.8 ± 21.4	79.7 ± 32.2 [*]	94.9 ± 34.7 ^{*,†}	<0.001
TAT, mL	6.49 ± 3.59	8.73 ± 4.94 [*]	8.95 ± 5.54 [*]	0.0282
AV groove fat, mm	9.72 ± 3.88	13 ± 5.65 [*]	16.13 ± 6.71 ^{*,†}	<0.001
IAF, mm	6.58 ± 1.78	8.44 ± 2.6 [*]	9.82 ± 2.85 ^{*,†}	<0.001

AV Groove = atrioventricular groove, BMI = body mass index, BNP = brain natriuretic peptide, eGFR = estimated glomerular filtration rate, HDL = high density apolipoprotein, HFpEF = heart failure with preserved ejection fraction, hs-CRP = high sensitivity C-reactive protein, IAF = inter-atrial fat, PCF = pericardial fat, TAT = thoracic periaortic.

^{*} $P < 0.05$ compared to healthy group.

[†] $P < 0.05$ compared to comorbidity group.

natriuretic peptide levels in both the comorbidity and HFpEF groups (both $P < 0.05$). We also observed that there was a graded increase in body fat composition, PCF, AV Groove Fat, and IAF across healthy, comorbidity, and HFpEF groups (all ANOVA $P < 0.05$), and subjects with higher metabolic scores consistently

showed greater visceral adiposity (Fig. 2, all $P < 0.05$). An age-, sex-, and BMI-matched study subgroup from the same cohort (total $n = 162$: $n = 27$, $n = 95$, and $n = 40$ in healthy, co-morbidity, and HFpEF groups, respectively) showed similar increase of visceral adiposity across the 3 groups, with AV Groove Fat and

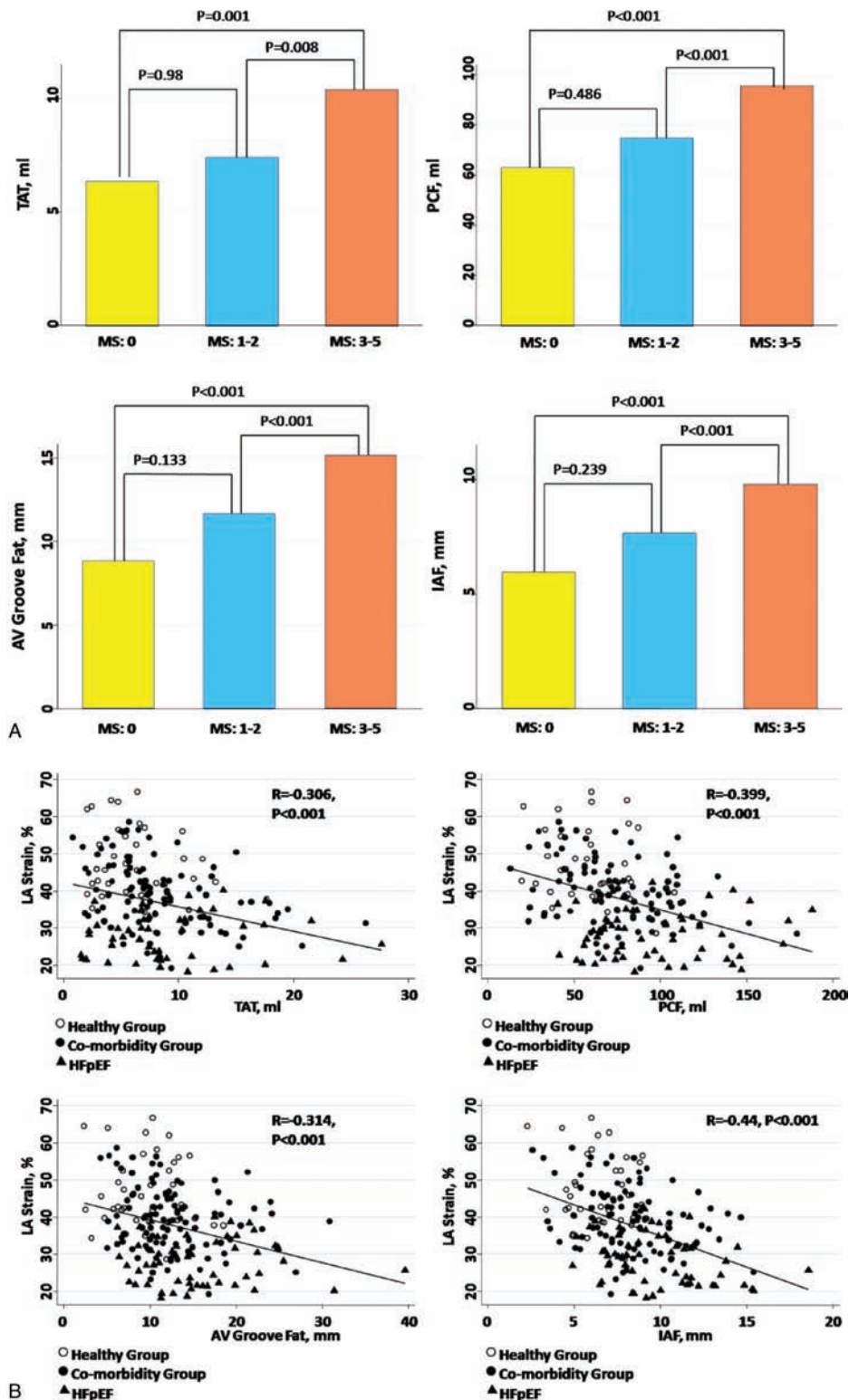


Figure 2. Comparisons of various adiposity measures among different metabolic score (MS) groups. Higher MSs were associated with a greater amount of various visceral adiposities accumulation, which is significantly larger in subjects with diagnosed metabolic syndrome compared with those with a smaller MS.

IAF differing substantially between comorbidity and HFpEF groups (Supplemental Material, Table 4, <http://links.lww.com/MD/B34>). Finally, a greater proportion of hypertension, diabetes mellitus, cardiovascular diseases, and medication use for hyperlipidemia was observed in both the comorbidity and HFpEF groups (all $P < 0.05$).

3.4. Baseline echocardiography indices in healthy, comorbidity, and HFpEF groups from outpatient clinic

Both comorbidity and HFpEF groups shared common features of cardiac phenotypic patterns, including greater LV wall thickness, larger LV mass, and greater degree of LV concentricity, although subjects categorized as HFpEF presented with smaller LV volumes (all $P < 0.05$) (Table 2). Diastolic function parameters appeared to be worse in both the comorbidity and HFpEF groups, with the HFpEF group demonstrating a greater degree of impaired LV diastolic relaxation, and higher LV filling pressures (both $P < 0.05$). Our study demonstrated that HFpEF groups had largest LA volumes and worst LA strains (-11.07% compared with comorbidity, $P < 0.001$), and the HFpEF group further showed a greater degree of LA stiffness (all $P < 0.05$). We also observed that both the comorbidity and HFpEF groups had similarly worsening longitudinal strain (-18.49% vs -15.7% , $P < 0.001$), and the HFpEF group further showed reduction in circumferential and radial strain when compared with the comorbidity and healthy groups (all $P < 0.05$). Finally, the trend toward various worse cardiac deformations and LA structural/

functional measures remained unchanged among groups after age, sex, and BMI matching (Supplemental Material, Table 4, <http://links.lww.com/MD/B34>).

3.5. The association between various adiposity measures and LA electromechanical parameters in healthy, comorbidity, and HFpEF groups from outpatient clinic

We observed that greater accumulation of various visceral adiposity measures (PCF, TAT, AV Groove Fat, and IAF, respectively) and greater body fat composition were inversely associated with LA mechanical function in terms of worsening strain ($r = -0.4, -0.31, -0.31, -0.44, \text{ and } -0.27$ for PCF, TAT, AV Groove Fat, IAF and body fat composition, respectively, all $P < 0.001$). A strong and consistent link between unfavorable LA electromechanical parameters and greater visceral fat deposits was shown, especially those in anatomic areas adjacent to the LA chamber (such as AV Groove Fat and IAF) after accounting for clinical covariates and profiles of MetS (Table 3, all $P < 0.05$). For each standardized unit increase of IAF, there was consistent reduction of LA strain (β -coef: -0.28 , 95% CI: -0.42 to -0.15), increase of LA stiffness (β -coef: 0.23 , 95% CI: 0.1 – 0.36), and more prolonged P wave duration (β -coef: 0.23 , 95% CI: 0.09 – 0.36 (all $P < 0.05$). Further, there was a trend toward greater corrected QT interval, P wave duration across healthy, comorbidity, and HFpEF groups (Supplemental Material, Table 5, P for trend < 0.05 , <http://links.lww.com/MD/B34>).

Table 2

Baseline echocardiography parameters in healthy, co-morbidity, and HFpEF groups (n=206).

Echocardiography measures	Healthy group (N = 40)	Comorbidity group (N = 108)	HFpEF group (N = 58)	P (trend)
Conventional echo parameters				
IVS, mm	9 ± 1.13	10.12 ± 1.54*	10.74 ± 1.27* [†]	<0.001
LVPW, mm	8.96 ± 1.1	9.96 ± 1.23*	10.79 ± 1.33* [†]	<0.001
LVEDV, mL	70.2 ± 15.6	74.6 ± 20.1	66.1 ± 16.1 [†]	<0.001
LVESV, mL	26.45 ± 7.03	27.53 ± 8.71	24.96 ± 8.11 [†]	0.397
LVEF, %	63.63 ± 5.72	63.5 ± 5.46	62.09 ± 6.34	0.238
RWT, %	39.8 ± 5.2	43.1 ± 7.1	46.9 ± 6.4*	<0.001
LV mass, g	135.79 ± 28.17	167.75 ± 34.93*	178.58 ± 39.97* [†]	<0.001
LV mass index, g/m ²	72.72 ± 13.59	85.85 ± 15.53*	90.86 ± 20.67* [†]	<0.001
LV mass-to-volume ratio	1.92 ± 0.68	2.1 ± 0.66*	2.79 ± 0.94* [†]	<0.001
Doppler indices				
Mitral E DT, ms	199.85 ± 51.48	232.39 ± 49.06*	234.43 ± 64.27* [†]	0.004
Mitral IVRT, ms	82.86 ± 15.94	99.7 ± 18.6*	85.81 ± 16.86 [†]	0.476
Mitral inflow E, cm/s	69.77 ± 15.9	66.06 ± 14.58*	77.32 ± 21.9* [†]	0.037
TDI E', cm/s	9.61 ± 2.03	7.82 ± 2.07*	5.86 ± 1.9* [†]	<0.001
E/E', mmHg	7.54 ± 2.3	9.07 ± 3.59	16.29 ± 6.33* [†]	<0.001
Left atrial indices				
LA volume (max), mL	30.5 ± 7.6	43 ± 8.2*	58.2 ± 11.2* [†]	<0.001
LA volume (min), ml	14 ± 4	20.4 ± 5.1*	31.3 ± 9.6* [†]	<0.001
LA strain, %	46.3 ± 9.6	39.2 ± 8.5*	28.2 ± 6.4* [†]	<0.001
LA stiffness, mmHg %	0.17 ± 0.05	0.24 ± 0.1	0.61 ± 0.29* [†]	<0.001
Deformation parameters				
Longitudinal strain, %	-19.86 ± 1.73	-18.49 ± 1.67	-15.7 ± 1.82* [†]	<0.001
Circumferential strain, %	-31.97 ± 4.34	-30.49 ± 4.82	-27.42 ± 5.33* [†]	<0.001
Radial strain, %	43.78 ± 12.33	40.04 ± 11.81	29.11 ± 7.8* [†]	<0.001
LV twist, degree	11.36 ± 3.26	12.99 ± 3.22	11.08 ± 2.74	0.674

DT = transmitral E-wave deceleration time, E = early mitral inflow diastolic velocity, E' = early mitral annular relaxation velocity, IVRT = iso-volumic relaxation time, IVS = inter-ventricular septum, LA = left atrial/left atrium, LV = left ventricular/left ventricle, LVPW = left ventricular posterior wall, S = strain.

* $P < 0.05$ compared to healthy group.

[†] $P < 0.05$ compared to comorbidity group.

Table 3**The associations between various adiposity measures and LA electromechanical parameters in Healthy, comorbidity, and HFpEF Groups (n = 206).**

Adiposity Measures	LA strain, %		LA stiffness index		P duration (corrected)	
	β -coef.	P	β -coef.	P	β -coef.	P
Univariate model						
Body fat composition, %	-0.274	<0.001	0.227	0.005	0.206	0.009
PCF, mL	-0.407	<0.001	0.353	<0.001	0.224	0.001
TAT, mL	-0.309	<0.001	0.223	0.003	0.152	0.032
AV groove fat, mm	-0.348	<0.001	0.343	<0.001	0.332	<0.001
IAF, mm	-0.443	<0.001	0.416	<0.001	0.41	<0.001
Multivariate model 1						
Body fat composition, %	-0.269	<0.006	0.203	0.006	0.201	0.006
PCF, mL	-0.373	<0.001	0.282	<0.001	0.174	0.008
TAT, mL	-0.305	<0.001	0.203	0.002	0.154	0.023
AV groove fat, mm	-0.309	<0.001	0.285	<0.001	0.299	<0.001
IAF, mm	-0.41	<0.001	0.341	<0.001	0.367	<0.001
Multivariate model 2						
Body fat composition, %	-0.071	0.371	0.08	0.326	0.064	0.425
PCF, mL	-0.218	0.006	0.206	0.008	0.034	0.673
TAT, mL	-0.103	0.246	0.16	0.063	0.006	0.964
AV groove fat, mm	-0.232	<0.001	0.266	<0.001	0.225	<0.001
IAF, mm	-0.33	<0.001	0.307	<0.001	0.286	<0.001
Multivariate model 3						
Body fat composition, %	-0.078	0.306	0.037	0.632	0.027	0.724
PCF, mL	-0.138	0.08	0.122	0.11	-0.049	0.529
TAT, mL	-0.054	0.536	0.083	0.333	-0.065	0.0449
AV groove fat, mm	-0.157	0.02	0.213	0.001	0.169	0.01
IAF, mm	-0.264	<0.001	0.265	<0.001	0.241	<0.001
Multivariate model 4						
Body fat composition, %	-0.073	0.338	0.051	0.525	0.032	0.674
PCF, mL	-0.138	0.077	0.151	0.047	-0.035	0.642
TAT, mL	-0.07	0.412	0.129	0.123	-0.04	0.632
AV groove fat, mm	-0.166	0.014	0.211	0.002	0.174	0.008
IAF, mm	-0.284	<0.001	0.227	0.001	0.225	0.001

Model 1: adjusted for age; Model 2: adjusted for age, sex, body mass index; Model 3: adjusted for age, sex, body mass index, systolic blood pressure, hypertension, diabetes, coronary artery disease, LV mass and eGFR; Model 4: adjusted for age, sex, body mass index, systolic blood pressure, LV mass, eGFR, and metabolic scores. AV Groove = atrioventricular groove, HFpEF = heart failure with preserved ejection fraction, IAF = inter-atrial fat, LA = left atrial/left atrium, PCF = pericardial fat, TAT = thoracic periaortic.

3.6. Risk stratification based on IAF adiposity measures in healthy, comorbidity, and HFpEF groups from outpatient clinic

Over a median 1017.8 days of follow-up (25th-75th: 683.5-1505 days), 29 subjects experienced HF-related hospitalization or death. We observed that larger IAF adiposity was related to higher incidence of HF hospitalization (hazard ratio [HR]: 3.71, 95% CI: 1.58-8.71), which remained significantly higher after adjusting for age, sex, and various echocardiography-derived parameters, including LV strain, LV mass index, and LV filling pressure as well as LA volumes (all $P < 0.05$). IAF above the median level (≥ 8.2 mm) carried nearly 4 times greater chance (HR: 4.11, 95% CI: 1.5-11.32, log rank $P < 0.05$) (Supplemental Material, Figure 1, <http://links.lww.com/MD/B34>) of having HF hospitalization even after adjusting age, sex, and LV mass index in survival model (Figure 3 & Supplemental Material, Table 6, <http://links.lww.com/MD/B34>). For the age-, sex-, and BMI-matched subgroup in the current work ($n = 162$), per standardized increase of IAF was associated with higher risk of HF hospitalization (HR: 2.67, 95% CI: 1.74-4.09, $P < 0.001$), which remained statistically significant after accounting for those echocardiography-derived evaluations.

4. Discussion

In our study, we showed that greater visceral adiposity measures were associated with unfavorable anthropometrics, worse cardiometabolic profiles, higher insulin resistance, and a greater degree of systemic inflammation. In addition, accumulation of visceral adipose deposits was related to certain cardiac remodeling and functional asynergy. Specifically, those fat deposits surrounding the atria were more relevant to LA electromechanical disturbances in terms of lower LA strain, higher LA stiffness, and interatrial conduction disturbances, which remained independent after accounting for baseline clinical covariates or medical histories. We also demonstrated that subjects with HFpEF featured an excessive burden of visceral adiposity, which may confer a higher risk for HF hospitalization during clinical follow-up.

Accumulating evidence supports the strong association of diabetes and obesity^[2,3] with HF incidence; those with MetS^[24] had higher rates of HF hospitalization.^[10] On one hand, MetS, defined as a constellation of several clinical components with a characteristic component of central obesity, is strongly linked to coronary artery disease^[25] and HF.^[10] On the other hand, the existence of MetS and insulin resistance as the relevant central factor has also been reported to mediate unbalanced

sympathovagal tone and regarded as proarrhythmic, in part driven by augmented oxidative stress, altered oxido-redox status, or regulative channels effect on ions, leading to altered electromechanical properties, higher rate of arrhythmia recurrence, and worse cardiovascular outcomes.^[26-28] Oxidative

stress itself had also been reported to play a role in regulating cardiac sympathetic innervations defect in HF, which further potentiate arrhythmia formation.^[29] Although the exact mechanisms underlying HF development in subjects with MetS remain unclear, a complex interplay of a variety factors and potential

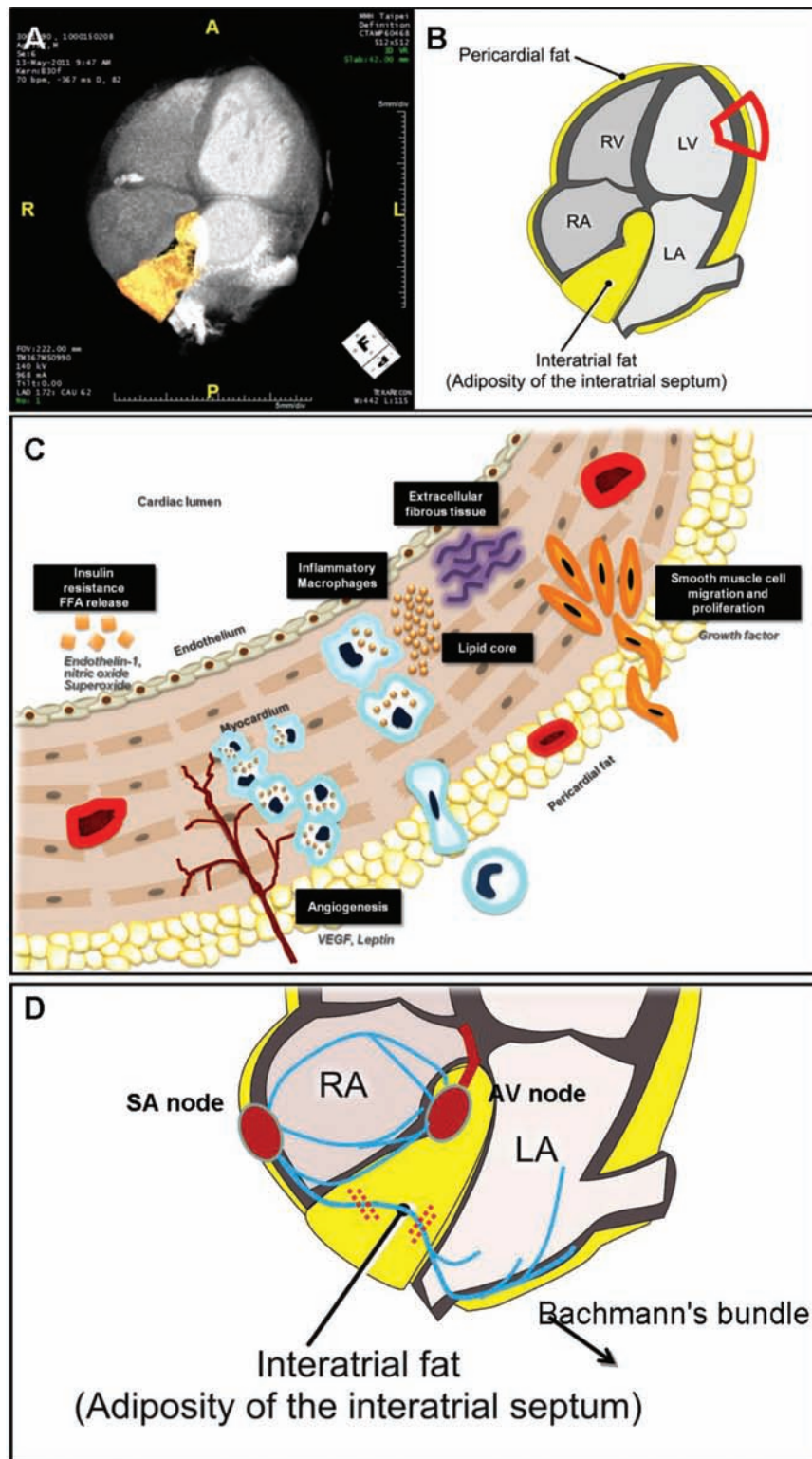


Figure 3. The schematic illustrations represented the location and assessment of various visceral adiposities surrounding cardiac structures (A, B), as well as the potential mechanisms and links among regional visceral adiposity measures, clinically observed metabolic derangements, elicited inflammation, and cardiac remodeling (C). The speculated mechanism of interatrial fat and associated left atrial cardiac electromechanical disturbances was also demonstrated.

pathogenesis are possibly involved (Supplemental Material, Figure 2, <http://links.lww.com/MD/B34>).^[8–10]

Central obesity or visceral adiposity, rather than subcutaneous or peripheral fat deposits, shows a consistent correlation with systemic inflammation and metabolic derangements, and had recently been regarded as the “key” biological sources of proinflammatory pathways and related adverse effects.^[13–15] So far, a variety of biomarkers, including brain natriuretic peptide family and insulin-like growth factor-I, have all been reported for HF risk stratification.^[30] Furthermore, circulating blood glucose, insulin resistance,^[31,32] and elevated inflammatory markers (e.g., interleukin-6 or hs-CRP) from systemic metabolic derangements were proposed to be associated with cardiac remodeling and redundant LV mass (Supplemental Material, Figure 2, <http://links.lww.com/MD/B34>).^[23] The term “cardiac steatosis” has recently been proposed to describe excessive myocardial triglyceride uptake, overflow of intramyocardial free fatty acids, enhanced beta oxidation, and a higher degree free radical accumulation within cardiomyocytes in diabetic subjects with HF,^[33–35] and further enhance oxidative stress and cardiac fibrosis (Fig. 3 A–C). Previous studies revealed that microvascular endothelial inflammation in metabolic derangements, rather than hemodynamic load, may further aggravate pathologic interstitial fibrosis and HF.^[36] Based on these findings, it has been proposed that visceral fat deposits could be biologically active and may exert cardiotoxic effects on adjacent cardiac structures, leading to cardiac functional deterioration.^[37,38] In this regard, HFpEF as a clinically distinct phenotype from reduced ejection fraction HF had been shown to be more relevant to such metabolic derangements and molecular proinflammatory signaling pathways.^[31–36] In accordance to previous data, our HFpEF group in the second-phase study indeed presented greater BMI and higher insulin resistance, as well as excessive visceral adiposity and more exaggerated systemic inflammation.

The same pathogenetic mechanisms underlying LV can also be applicable to LA. LA functional decline as well as structural remodeling or dilation may occur in subjects with HF and elevated cardiac filling pressures.^[39] However, LA fibrosis or remodeling secondary to comorbidities including hypertension, diabetes, obesity, or ischemia may pathologically resemble LV subendocardial damage though inflammatory responses independent of elevated filling pressures.^[33,40–42] Such LA fibrotic changes may lead to increased LA stiffness with concomitant mechanical failure, leading to “stiff LA syndrome,” which could be more evident in HFpEF when compared to those with hypertensive hypertrophy.^[4,5] By utilizing deformation measures, we are now capable of identifying LA functional abnormalities without volume expansion or remodeling in subjects with HF. Furthermore, the disease entity “lipomatous hypertrophy” and findings from several large epidemiological studies have shown that altered LA electrical properties or conduction disturbances were associated with excessive PCF,^[43] which may also result in initiation and perpetuation of AF.^[18,44–45] Taken together, these data may indicate that IAF accumulation may also impede interatrial conduction at a later stage, which may be partly driven by its anatomic proximity to specialized interatrial conduction fibers (Fig. 3 D). Of note, although body fat composition is a commonly used clinical tool for total body adiposity assessment,^[46] we showed in our work that its association with LA electromechanical indexes became markedly attenuated after accounting for BMI. This finding may also support our speculations that regional adiposity burden may differ from global fat assessment in several biological behaviors.

We therefore speculate that IAF may be an alternative, new, and representative surrogate marker of visceral fat in addition to the pericardial adiposity measure, as the latter assessment remains exclusively confined to pericardial sac with minimal expansion capacity during clinical progression of metabolic derangements in the same individual. Finally, we show in our work that such visceral adipose tissue is readily assessable using noninvasive imaging methods, which are more practical for clinical use in daily practice.

4.1. Limitations

A number of limitations may exist in our current work. First, our findings are cross-sectional. Despite our inability to establish causal relationship from our data, we believe that these findings could supplement observations with metabolic derangements and obesity as a major clinical risk in the pathogenesis of HF, especially for those with HFpEF. Therefore, the real causes and cause–effect relationship between IAF deposits and worsening LA electromechanical function may warrant further investigations. In addition, comparisons of these visceral fat depots between more “diseased” individuals and a healthy control group with clinically fully matched baseline demographics (such as age or body size in terms of BMI) may be difficult, and the real effect of visceral adiposity on cardiac functions and its prognostic value will have to be interpreted with caution in our current work. Therefore, further work may be helpful to solve these puzzles. Finally, while the somewhat different recruiting periods in various study phases might induce a bias in the patients’ selection, though there were no major changes in our clinical practice and settings during these study periods.

5. Conclusion

Greater visceral adiposity measures are positively correlated with several cardiometabolic derangements, insulin resistance, and elicited inflammatory response. In addition, subjects with known clinical cardiovascular risks or diagnosed HFpEF were prone to present with greater degrees of visceral adiposity and higher degree of metabolic abnormalities. Excessive accumulation of visceral adiposity, especially IAF deposition, may likely mediate several adverse biological effects or pathologies, resulting in a broad spectrum of LA electromechanical disturbances. Finally, greater accumulation of such visceral adiposity was also related to higher rates of HF hospitalization.

Acknowledgements

We especially would like to extend our gratitude to Bernard and Kuo-Tzu Sung for their great efforts and contribution to the graphs and illustrations in this work.

References

- [1] Melenovsky V, Borlaug BA, Rosen B, et al. Cardiovascular features of heart failure with preserved ejection fraction versus nonfailing hypertensive left ventricular hypertrophy in the urban Baltimore community: the role of atrial remodeling/dysfunction. *J Am Coll Cardiol* 2007;49:198–207.
- [2] Welles CC, Ku IA, Kwan DM, et al. Left atrial function predicts heart failure hospitalization in subjects with preserved ejection fraction and coronary heart disease: longitudinal data from the Heart and Soul Study. *J Am Coll Cardiol* 2012;59:673–80.
- [3] Kuppahally SS, Akoum N, Burgon NS, et al. Left atrial strain and strain rate in patients with paroxysmal and persistent atrial fibrillation. Relationship to left atrial structural remodeling detected by delayed-enhancement MRI. *Circ Cardiovasc Imaging* 2010;3:231–9.

- [4] Tan YT, Wenzelburger F, Lee E, et al. Reduced left atrial function on exercise in patients with heart failure and normal ejection fraction. *Heart* 2010;96:1017–23.
- [5] Kurt M, Wang J, Torre-Amione G, et al. Left atrial function in diastolic heart failure. *Circ Cardiovasc Imaging* 2009;2:10–5.
- [6] Kokubu N, Yuda S, Tsuchihashi K, et al. Noninvasive assessment of left atrial function by strain rate imaging in patients with hypertension: a possible beneficial effect of renin-angiotensin system inhibition on left atrial function. *Hypertens Res* 2007;30:13–21.
- [7] Kannel WB, Hjortland M, Castelli WP. Role of diabetes in congestive heart failure: the Framingham study. *Am J Cardiol* 1974;34:29–34.
- [8] van Heerebeek L, Hamdani N, Handoko ML, et al. Diastolic stiffness of the failing diabetic heart: importance of fibrosis, advanced glycation end products, and myocyte resting tension. *Circulation* 2008;117:43–51.
- [9] Witteles RM, Fowler MB. Insulin-resistant cardiomyopathy: clinical evidence, mechanisms, and treatment options. *J Am Coll Cardiol* 2008;51:93–102.
- [10] Horwich TB, Fonarow GC. Glucose, obesity, metabolic syndrome, and diabetes relevance to incidence of heart failure. *J Am Coll Cardiol* 2010;26:283–93. 55.
- [11] Watanabe H, Tanabe N, Watanabe T, et al. Metabolic syndrome and risk of development of atrial fibrillation: the Niigata preventive medicine study. *Circulation* 2008;117:1255–60.
- [12] Edelmann F, Wachter R, Schmidt AG, et al. Effect of spironolactone on diastolic function and exercise capacity in patients with heart failure with preserved ejection fraction: the Aldo-DHF randomized controlled trial. *JAMA* 2013;309:781–91.
- [13] Kumar A, Thota V, Dee L, et al. Tumor necrosis factor alpha and interleukin 1beta are responsible for in vitro myocardial cell depression induced by human septic shock serum. *J Exp Med* 1996;183:949–58.
- [14] Han JM, Levings MK. Immune regulation in obesity-associated adipose inflammation. *J Immunol* 2013;191:527–32.
- [15] Van Tassel BW, Toldo S, Mezzaroma E, et al. Targeting interleukin-1 in heart disease. *Circulation* 2013;128:1910–23.
- [16] Liao ZY, Peng MC, Yun CH, et al. Relation of carotid artery diameter with cardiac geometry and mechanics in heart failure with preserved ejection fraction. *J Am Heart Assoc* 2012;1:e003053.
- [17] Nichols JH, Samy B, Nasir K, et al. Volumetric measurement of pericardial adipose tissue from contrast-enhanced coronary computed tomography angiography: a reproducibility study. *J Cardiovasc Comput Tomogr* 2008;2:288–95.
- [18] Shin SY, Yong HS, Lim HE, et al. Total and Inter-atrial epicardial adipose tissues are independently associated with left atrial remodeling in patients with atrial fibrillation. *J Cardiovasc Electrophysiol* 2011;22:647–55.
- [19] Grundy SM, Brewer HBJr, Cleeman JI, et al. American Heart Association; National Heart, Lung, and Blood Institute. Definition of metabolic syndrome: Report of the National Heart, Lung, and Blood Institute/American Heart Association conference on scientific issues related to definition. *Circulation* 2004;109:433–8.
- [20] Fan JG, Saibara T, Chitturi S, et al. What are the risk factors and settings for non-alcoholic fatty liver disease in asia-pacific? *J Gastroenterol Hepatol* 2008;22:794–800.
- [21] Dekker JM, Girman C, Rhodes T, et al. Metabolic syndrome and 10-year cardiovascular disease risk in the Hoorn Study. *Circulation* 2005;112:666–73.
- [22] Bazett HC. The time relations of the blood-pressure changes after excision of the adrenal glands, with some observations on blood volume changes. *J Physiol* 1920;53:320–9.
- [23] Morris DA, Gailani M, Vaz Pérez A, et al. Left atrial systolic and diastolic dysfunction in heart failure with normal left ventricular ejection fraction. *J Am Soc Echocardiogr* 2011;24:651–2.
- [24] Bahrami H, Blumenthal DA, Kronmal R, et al. Novel metabolic risk factors for incident heart failure and their relationship with obesity: the MESA (Multi-Ethnic Study of Atherosclerosis) study. *J Am Coll Cardiol* 2008;6:1775–83. 51.
- [25] Suzuki T, Katz R, Jenny NS, et al. Metabolic syndrome, inflammation, and incident heart failure in the elderly: the cardiovascular health study. *Circ Heart Fail* 2008;1:242–8.
- [26] Rizzo MR, Sasso FC, Marfella R, et al. Autonomic dysfunction is associated with brief episodes of atrial fibrillation in type 2 diabetes. *J Diabetes Complications* 2015;29:88–92.
- [27] Sardu C, Carreras G, Katsanos S, et al. Metabolic syndrome is associated with a poor outcome in patients affected by outflow tract premature ventricular contractions treated by catheter ablation. *BMC Cardiovasc Disord* 2014;14:176.
- [28] Marfella R, Sasso FC, Siniscalchi M, et al. Brief episodes of silent atrial fibrillation predict clinical vascular brain disease in type 2 diabetic patients. *J Am Coll Cardiol* 2013;62:525–30.
- [29] Marfella R, Barbieri M, Sardu C, et al. Effects of α -lipoic acid therapy on sympathetic heart innervation in patients with previous experience of transient takotsubo cardiomyopathy. *J Cardiol* 2016;67:153–61.
- [30] Petretta M, Colao A, Sardu C, et al. NT-proBNP, IGF-I and survival in patients with chronic heart failure. *Growth Horm IGF Res* 2007;17:288–96.
- [31] Grundy SM, Cleeman JI, Daniels SR, et al. Diagnosis and management of the metabolic syndrome: an American Heart Association/National Heart, Lung, and Blood Institute Scientific Statement. *Circulation* 2005;112:2735.
- [32] Verdecchia P, Reboldi G, Schillaci G, et al. Circulating insulin and insulin growth factor-1 are independent determinants of left ventricular mass and geometry in essential hypertension. *Circulation* 1999;100:1802–7.
- [33] Fujita M, Asanuma H, Kim J, et al. Impaired glucose tolerance: a possible contributor to left ventricular hypertrophy and diastolic dysfunction. *Int J Cardiol* 2007;118:76–80.
- [34] Lam CS, Donal E, Kraigher-Krainer E, et al. Epidemiology and clinical course of heart failure with preserved ejection fraction. *Eur J Heart Fail* 2011;13:18–28.
- [35] Dhoble A, Patel MB. Cardiac steatosis and myocardial dysfunction. *J Am Coll Cardiol* 2009;53:636.
- [36] Rijzewijk LJ, van der Meer RW, Smit JW, et al. Myocardial steatosis is an independent predictor of diastolic dysfunction in type 2 diabetes mellitus. *J Am Coll Cardiol* 2008;52:1793.
- [37] Paulus WJ, Tschöpe C. A novel paradigm for heart failure with preserved ejection fraction: comorbidities drive myocardial dysfunction and remodeling through coronary microvascular endothelial inflammation. *J Am Coll Cardiol* 2013;62:263–71.
- [38] McGavock JM, Victor RG, Unger RH. Szczepaniak LS; American College of Physicians and the American Physiological Society. Adiposity of the heart, revisited. *Ann Intern Med* 2006;144:517–24.
- [39] van Heerebeek L, Hamdani N, Falcão-Pires I, et al. Low myocardial protein kinase G activity in heart failure with preserved ejection fraction. *Circulation* 2012;126:830–9.
- [40] Paulus WJ, Tschöpe C, Sanderson JE, et al. How to diagnose diastolic heart failure: a consensus statement on the diagnosis of heart failure with normal left ventricular ejection fraction by the Heart Failure and Echocardiography Associations of the European Society of Cardiology. *Eur Heart J* 2007;28:2539–0.
- [41] Burstein B, Nattel S. Atrial fibrosis: mechanisms and clinical relevance in atrial fibrillation. *J Am Coll Cardiol* 2008;51:802–9.
- [42] Iacobellis G, Corradi D, Sharma AM. Epicardial adipose tissue: anatomic, biomolecular and clinical relationships with the heart. *Nat Clin Pract Cardiovasc Med* 2005;2:536–43.
- [43] Babcock MJ, Soliman EZ, Ding J, et al. Pericardial fat and atrial conduction abnormalities in the Multiethnic Study of Atherosclerosis (MESA). *Obesity* 2011;19:179–84.
- [44] Shirani J, Roberts WC. Clinical electrocardiographic and morphologic features of massive fatty deposits (“lipomatous hypertrophy”) in the atrial septum. *J Am Coll Cardiol* 1993;22:226–38.
- [45] Muranaka A, Yuda S, Tsuchihashi K, et al. Quantitative assessment of left ventricular and left atrial functions by strain rate imaging in diabetic patients with and without hypertension. *Echocardiography* 2009;26:262–71.
- [46] Cornier MA, Després JP, Davis N, et al. American Heart Association Obesity Committee of the Council on Nutrition; Physical Activity and Metabolism; Council on Arteriosclerosis; Thrombosis and Vascular Biology; Council on Cardiovascular Disease in the Young; Council on Cardiovascular Radiology and Intervention; Council on Cardiovascular Nursing, Council on Epidemiology and Prevention; Council on the Kidney in Cardiovascular Disease, and Stroke Council. Assessing adiposity: a scientific statement from the American Heart Association. *Circulation* 2011;124:1996–2019.